International Journal of Fluid Machinery and Systems
Vol. 4, No. 1, January-March 2011

DOI: 10.5293/IJFMS.2011.4.1.114
ISSN (Online): 1882-9554

Original Paper (Invited)

Theory and Prediction of Turbulent Transition

Hua-Shu Dou[1] and Boo Cheong Khoo[2]

[1]Temasek Laboratories, National University of Singapore,
Singapore 117411
tsldh@nus.edu.sg, huashudou@yahoo.com
[2]Department of Mechanical Engineering, National University of Singapore,
Singapore 119260
mpekbc@nus.edu.sg

Abstract

We have proposed a new approach based on energy gradient concept for the study of flow instability and turbulent transition in parallel flows in our previous works. It was shown that the disturbance amplitude required for turbulent transition is inversely proportional to Re, which is in agreement with the experiments for imposed transverse disturbance. In present study, the energy gradient theory is extended to the generalized curved flows which have much application in turbomachinery and other fluid delivery devices. Within the frame of the new theory, basic theorems for flow instability in general cases are provided in details. Examples of applications of the theory are given from our previous studies which show comparison of the theory with available experimental data. It is shown that excellent agreement has been achieved for several configurations. Finally, various prediction methods for turbulent transition are reviewed and commented.

Keywords: Turbulent transition; Mechanism; Theory; Theorem; Prediction.

1. Introduction

Turbulence is still a challenging problem in science and engineering even though much effort of more than a century has been made in the science community since the pioneering work of Reynolds (1883) [1-5]. In practice, the understanding of turbulence transition and generation has great significance for basic sciences and many engineering fields such as aerospace, mechanical, environmental, energy and chemical engineering, etc. This issue is intricately related to the instability problem of the base flow subjected to some imposed disturbances [1-2].

In the past, several stability theories have been developed to describe the mechanism of flow instability. These are: (1) The linear stability theory, which goes back to Rayleigh (1880), is a widely used method and has been applied to several problems [6]. For Taylor-Couette flow and Rayleigh-Bernard convective problem, it agrees well with experimental data. However, this theory fails when used for wall-bounded parallel flows such as plane Couette flow, plane Poiseuille flow and pipe Poiseuille flow. (2) The energy method (Orr, 1907) which is based on the Reynolds-Orr equation is another mature method for estimating flow instability [7]. However, agreement could not be obtained between the theoretical predictions and the experiment data. (3) The weakly nonlinear stability theory (Stuart, 1971) emerged in 1960's and the application is very limited (see [8]). (4) The secondary instability theory (Herbert et al, 1988), which was developed most recently, explains some of flow transition phenomena (mainly for the boundary layer flow) better than the other earlier theories (see [9]). However, there are still significant discrepancies between the predictions obtained using this method and experimental data; particularly at transition.

Stability of parallel flows is the fundamental of stability studies (Fig.1). This topic has attracted many scientists to explore the physics of turbulent transition for more than 60 years since the pioneering work of Lin [2]. For plane Poiseuille flow, Lin demonstrated by asymptotic analysis that the flow is unstable when the Re exceeds 8000 [2]. However, how this instability is related to turbulent transition was not studied. Subsequently, more careful numerical studies showed that this critical value of Re based on linear stability is 5772 for plane Poiseuille flow, see [1]. For wall bounded parallel flows, it is observed from experiments that there is a critical Reynolds number Re_c below which no turbulence can be sustained regardless of the level of imposed disturbance. For the pipe Poiseuille flow, this critical value of Reynolds number is about 2000 as found from experiments [10,11]. Above this Re_c, the transition to turbulence depends to a large extent on the initial disturbance to the flow. For example,

Accepted for publication December 19, 2010: Paper number O10051S
Corresponding author: Hua-Shu Dou, Research Scientist, huashudou@yahoo.com; tsldh@nus.edu.sg

This paper was presented at 2010 International Conference on Pumps and Fans, October 18-21, 2010, Hangzhou, China

experiments showed that if the disturbances in a laminar flow can be carefully avoided or considerably reduced, the onset of turbulence can be delayed to Reynolds number up to Re=O(10^5), see [12]. Experiments also showed that for Re> Re_c, only when a threshold of disturbance amplitude is reached, can the flow transition to turbulence occur [13]. Trefethen et al. suggested that the critical amplitude of the disturbance leading to transition varies broadly with the Reynolds number and is associated with an exponent rule of the form, $A \propto \mathrm{Re}^{\gamma}$ [12]. The magnitude of this exponent has significant implication for turbulence research [12]. Chapman, through a formal asymptotic analysis of the Navier-Stokes equations (for $\mathrm{Re} \to \infty$), found $\gamma = -3/2$ and -5/4 for plane Poiseuille flow with streamwise mode and oblique mode, respectively, with generating a secondary instability, and $\gamma = -1$ for plane Couette flow applicable to the above-mentioned both modes. He also examined the boot-strapping route to transition without needing to generate a secondary instability, and found $\gamma = -1$ for both plane Poiseuille flow and plane Couette flow [14]. Recently, Hof et al. [15], used pulsed injection disturbances in experiments, to obtain the normalized disturbance flow rate in the pipe for the turbulent transition, and found it to be inversely proportional to the Re number, i.e., $\gamma = -1$. Further experiments later confirmed this scaling law for transverse injection disturbance [16], while the value of γ is not -1 for no- transverse injection disturbance. These experimental results mean that the product of the amplitude of the disturbance and the Reynolds number may be important for the consideration of transition to turbulence. This phenomenon must ultimately have a physical background, and a physical mechanism for this result was proposed by Dou [17,18].

Dou [17,18] proposed an *energy gradient theory* with the aim of clarifying the mechanism of flow transition from laminar flow to turbulence. He gave detailed derivations for this method based on first principle Newton's mechanics, and thus it is compatible with the Navier-Stokes equations. For plane Poiseuille flow and Hagen-Poiseuille flow, this method yields consistent results with experimental data. This method is also used to explain the mechanism of instability of inflectional velocity profile for viscous flow and this inflectional instability is only valid for pressure driven flows (it should be noticed that inflectional instability is not suitable for plane Couette flow). However, for shear driven flows such as plane Couette flow, the situation is changed since the energy loss could not be obtained directly from the Navier-Stokes equations. It should be mentioned that the energy gradient method is a semi-empirical theory based on physical analysis since the critical value of K is observed experimentally and cannot be directly calculated from the theory thus far.

In this paper, the basic principle of this method is generalized for curved flows. The basic theorems for flow instability in general cases are provided. Comparisons of the theory with experimental data are given (excellent agreement is achieved for all the available published data). Based on these results, the prediction methods for turbulent transition are reviewed.

2. Energy Gradient Method for Curved Flows

The energy gradient theory has been described for parallel flows in detail in [17,18]. Extending the theory from parallel flow to curved flow (Fig.2 and Fig.3), we only need to change the Cartesian coordinates (x, y) to curvilinear coordinates (s, n), to replace the kinetic energy ($\frac{1}{2}mu^2$) with the total mechanical energy ($E = p + (1/2)\rho u^2$), and to make the velocity (u) along the streamline. Here, we use the similar steps in the derivation to those in [18].

Let us consider the *elastic* collision of particles when a disturbance is imposed to the base of a curved shear flow (Fig.3). A fluid particle P at its equilibrium position will move in a cycle in the vertical direction under a vertical disturbance, and it will have two collisions with two particles (P_1 and P_2) at its maximum disturbance distances, respectively. The masses of the three particles are m, m_1 and m_2, and the corresponding velocities prior to collisions are u, u_1 and u_2. We shall use primes for the corresponding quantities after collision. Without loss of generality, we may assume $m = m_1 = m_2$ for convenience of the derivation. For parallel flows, only kinetic energy difference exists between neighboring streamlines. For curved flows, the difference of energy between streamlines is the difference of the total mechanical energy. When fluid particles exchange energy by collisions, it is the exchange of the total mechanical energy. For a cycle of disturbances, the fluid particle may absorb energy by collision in the first half-period and it may release energy in the second half-period because of the gradient of the total mechanical energy. The total momentum and total mechanical energy are conserved during the elastic collisions. The conservation equations for the first collision on streamline S_1 are

$$m_1 u_1 + mu = m_1 u'_1 + mu' = \alpha_1 (m_1 + m) u_1, \tag{1}$$

and

$$Q_1 E_1 + QE = Q_1 E'_1 + QE' = \beta_1 (Q_1 + Q) E_1. \tag{2}$$

Here $Q = m/\rho$ and $Q_1 = m_1/\rho$ are the volumes of the particles, and α_1 and β_1 are two constants such that $\alpha_1 \le 1$ and $\beta_1 \le 1$. The values of α_1 and β_1 are related to the residence time of the particle at P_1. If the residence time at position P_1 is sufficiently long (e.g. whole half-period of disturbance), the particle P would have undergone a large number of collisions with other particles on this streamline and would have the same momentum and total mechanical energy as those on the line of S_1, and it is required that α_1 =1 and β_1 =1. In this case, the energy gained by the particle P in the half-period is ($QE_1 - QE$). When the particle P remains on S_1 for less than the necessary half-period of the disturbance, the energy gained by the particle P can be written as $\beta^*_1 (QE_1 - QE)$, where β^*_1 is a fraction of a half-period with $\beta^*_1 < 1$.

The requirements of conservation of momentum and energy should also be applied for the second collision on streamline S_2, and similar equations to Eq.(1) and (2) can be obtained as in [17,18]. The difference is that the energy gained in the second half-cycle is negative owing to the distribution of energy in base flow. For the first half-period, the particle gains energy by the collision and the particle also releases energy by collision in the second half-period.

We use the (s, n) to express the coordinates in streamwise and transverse directions, respectively. Using the similar derivations to those in [18], the energy variation per unit volume of fluid for a half-period for the disturbed fluid particles can be obtained as,

$$\Delta E = \frac{2}{T}\int_0^{T/2}\frac{\partial E}{\partial n}n dt = \frac{\partial E}{\partial n}\frac{2}{T}\int_0^{T/2} n dt, \tag{3}$$

where $E = p + (1/2)\rho u^2$ is the total mechanical energy per unit volume of fluid, and T is the period.

Without loss of generality, we shall assume that the disturbance variation is associated with a sinusoidal function,

$$n = A\sin(\omega t + \varphi_0) \tag{4}$$

where *A* is the amplitude of disturbance in transverse direction, ω is the frequency of the disturbance, *t* is the time, and φ_0 is the initial phase angle. For the curved flow, A is respectively expressed by A_1 and A_2 in the first half and the second half circle; generally, $A_1 \neq A_2$. The velocity of the disturbance in the vertical direction, is the derivative of (4) with respect to time,

$$v' = \frac{dn}{dt} = v'_m \cos(\omega t + \varphi_0). \tag{5}$$

Here, $v'_m = A\omega$ is the amplitude of disturbance velocity and the disturbance has a period of $T = 2\pi/\omega$.

Substituting Eq.(4) into Eq. (3), we obtain the energy variation per unit volume of fluid for the first half-period,

$$\Delta E = \frac{\partial E}{\partial n}\frac{2}{T}\int_0^{T/2} n dt = \frac{\partial E}{\partial n}\frac{2}{T}\int_0^{T/2} A\sin(\omega t + \varphi_0)dt = \frac{\partial E}{\partial n}\frac{2}{T}\frac{1}{\omega}\int_0^{\pi} A\sin(\omega t + \varphi_0)d\omega t = \frac{\partial E}{\partial n}\frac{2A}{\pi}. \tag{6}$$

The stability of the particle can be related to the energy gained by the particle through vertical disturbance and the energy loss due to viscosity along streamline in a half-period.

The energy loss per unit volume of fluid along the streamline due to viscosity in a half-period is obtained in a similar way as in [18],

$$\Delta H = \frac{\partial H}{\partial s} l = \frac{\partial H}{\partial s}\frac{\pi}{\omega}u. \tag{7}$$

where *H* is the energy loss per unit volume of fluid due to viscosity along the streamline, $l = u(T/2) = u(\pi/\omega)$ is streamwise length moved by the particle in a half-period.

The magnitudes of ΔE and ΔH determine the stability of the flow. After the particle moves a half cycle, if the net energy gained by collisions is zero, this particle will stay in its original equilibrium position (streamline). If the net energy gained by collisions is larger than zero, this particle will be able to move into equilibrium with a higher energy state. If the collision in a half-period results in a drop of total mechanical energy, the particle can move into lower energy equilibrium. However, there is a critical value of energy increment which is balanced (damped) by the energy loss due to viscosity. When the energy increment accumulated by the particle is less than this critical value, the particle could not leave its original equilibrium position after a half-cycle. Only when the energy increment accumulated by the particle exceeds this critical value, could the particle migrate to its neighbor streamline and its equilibrium will become unstable.

The stability of a flow depends on the relative magnitude of ΔE and ΔH. For flow with a curved streamline, with similar steps as in [18], the relative magnitude of the energy gained from collision and the energy loss due to viscous friction determines the disturbance amplification or decay. Thus, for a given flow, a stability criterion can be written as below for the half-period, via Eq.(6) and Eq.(7),

$$F = \frac{\Delta E}{\Delta H} = \left(\frac{\partial E}{\partial n}\frac{2A}{\pi}\right)\Big/\left(\frac{\partial H}{\partial s}\frac{\pi}{\omega}u\right) = \frac{2}{\pi^2}K\frac{A\omega}{u} = \frac{2}{\pi^2}K\frac{v'_m}{u} < Const, \tag{8}$$

and

$$K = \frac{\partial E / \partial n}{\partial H / \partial s}. \tag{9}$$

Here, F is a function of coordinates which expresses the ratio of the energy gained by the particle in a half-period and the energy loss due to viscosity in the half-period. K is a dimensionless field variable (function) and expresses the ratio of transversal energy gradient and the rate of the energy loss along the streamline. Here, $E = p + (1/2)\rho V^2$ is the total mechanical energy, s is along the streamwise direction and n is along the transverse direction.

It can be found from Eq.(8) that the instability of a flow depends on the value of K and the amplitude of the relative disturbance velocity v'_m / u. For given disturbance, the maximum of K, K_{max}, in the flow domain determines the stability. Therefore, K_{max} is taken as a stability parameter here. For $K_{max}<K_c$, the flow is stable; for $K_{max}>K_c$, the flow is unstable. Here, K_c is the critical value of K_{max}. For all types of flows, it has been shown that the magnitude of K is proportional to the global Reynolds number for a given geometry [17,18]. Thus, the criterion of Eq.(8) can be written as,

$$\mathrm{Re}\frac{v'_m}{u} < Const. \tag{10}$$

For a given flow geometry, U is a characteristic velocity and generally is a function of u. Thus, Eq.(10) can be written as,

$$\mathrm{Re}\frac{v'_m}{U} < Const, \tag{11}$$

$$\text{or} \quad (\frac{v'_m}{U})_c \sim (\mathrm{Re})^{-1}. \tag{12}$$

Thus, it is found from Eq.(8) that the critical amplitude of the disturbance scales with the Re by an exponent of -1. This scaling has been confirmed by careful experiments for pipe flow in [17,18].

This theory obtains good agreement with the experiments in parallel flows in three aspects [17,18]. (1) The threshold amplitude of disturbance for transition to turbulence is scaled with Re by an exponent of -1 in parallel flows (Fig.4), which explains the recent experimental results of pipe flow by Hof et al. [15] and also Peixinho and Mullin [16] where injection disturbances are used. (2) For wall bounded parallel flows, turbulent transition takes place at a critical value of the energy gradient parameter, K_{max}, about 370-380, below which no turbulence exists. (3) The location where the flow instability is first initiated accords with the experiments. This location is at y/h=0.58 for plane Poiseuille flow and at r/R=0.58 for pipe Poiseuille flow, which have been confirmed by Nishioka et al's [19] experiments and Nishi et al's [20] experiments, respectively.

3. Three Important Theorems on Flow Stability For Curved Flows

In our previous work, we have applied the energy gradient theory to derive the three important theorems on flow stability for curved flows [21]. In this section, we give the details of the formulation of these theorems.

The equation of total mechanical energy for incompressible flow by neglecting the gravitational energy can be written as [17,18],

$$\rho\frac{\partial \mathrm{u}}{\partial t} + \nabla(p + \frac{1}{2}\rho u^2) = \mu\nabla^2 \mathrm{u} + \rho(\mathrm{u}\times\nabla\times\mathrm{u}). \tag{13}$$

For pressure driven flows, the derivatives of the total mechanical energy in the transverse direction and the streamwise direction can be expressed, respectively, as [21],

$$\frac{\partial E}{\partial n} = \frac{\partial(p + (1/2)\rho u^2)}{\partial n} = \rho(\mathrm{u}\times\omega)\cdot\frac{d\mathrm{n}}{|d\mathrm{n}|} + (\mu\nabla^2\mathrm{u})\cdot\frac{d\mathrm{n}}{|d\mathrm{n}|} = \rho u\omega + (\mu\nabla^2\mathrm{u})_n \tag{14}$$

$$\frac{\partial E}{\partial s} = \frac{\partial(p + (1/2)\rho u^2)}{\partial s} = \rho(\mathrm{u}\times\omega)\cdot\frac{d\mathrm{s}}{|d\mathrm{s}|} + (\mu\nabla^2\mathrm{u})\cdot\frac{d\mathrm{s}}{|d\mathrm{s}|} = (\mu\nabla^2\mathrm{u})_s, \tag{15}$$

where $\omega = \nabla\times\mathrm{u}$ is the vorticity. Since there is no work input in the pressure driven flows, the magnitude of the total mechanical energy loss of unit volumetric fluid along the streamwise direction equals to the derivatives of the total mechanical energy in the streamwise directions. That is [22],

$$\frac{\partial H}{\partial s} = -\frac{\partial E}{\partial s}. \tag{16}$$

For shear driven flows, the derivatives of the total mechanical energy in the transverse direction is the same as Eq.(14). The energy loss of unit volumetric fluid along the streamwise direction equals to the derivatives of the total mechanical energy in the streamwise directions plus the work done to the fluid by the external,

$$\frac{\partial H}{\partial s} = -\frac{\partial E}{\partial s} + \frac{\partial W}{\partial s}, \tag{17}$$

where *W* is the work done to the unit volume fluid by the external.

It is found from Eq.(14) that the transversal energy gradient is composed of two parts: the vorticity flux and the viscous diffusion of transversal velocity. For parallel flows, the transversal velocity is zero, v=0 and there is no viscous diffusion of transversal velocity, $(\mu\nabla^2 \mathrm{u})_n = 0$. The energy gradient in transverse direction is $\frac{\partial E}{\partial n} = \rho u \omega$. Viscosity only induces viscous loss of energy, $(\mu\nabla^2 \mathrm{u})_s$. Thus, viscosity plays the part of stability in parallel flows (e.g., free shear layer, pipe Poiseuille flow, plane Poiseuille flow, and plane Coutte flow). This characterization is a significant difference between parallel and non-parallel flows, which may result in variations of flow phenomena between them. It should be noted that the boundary layer flow on a flat plate is not a parallel flow, and therefore, there exists viscous diffusion of transversal velocity. This viscous diffusion can change the energy distribution and leads to (possibly) more unstable role if it increases the value of K according to "energy gradient theory." For circular flows, similar to parallel flows, there is no viscous diffusion of transversal velocity too. Viscosity has only the role of stabilization. This behaviour has been confirmed in Taylor-Couette flows between concentric rotating cylinders. As such, we may obtain (for viscous flow only):

Corollary (1): Viscosity has only the role of stabilization in parallel flows.
Corollary (2): Viscosity has only the role of stabilization in circular flows.

In the following, we shall prove three important theorems for flow stability [21].

Theorem (1): Potential flow (inviscid and $\nabla \times \mathrm{u} = 0$) is stable.

Proof: For inviscid flow, there is no energy loss along the streamline due to absence of viscosity. From Eqs.(15) and (16), we have

$$\frac{\partial H}{\partial s} = 0. \tag{18}$$

The energy gradient in the transverse direction for potential flow is zero due to $\omega = 0$, from Eq.(14)

$$\frac{\partial E}{\partial n} = \frac{\partial (p + 1/2\rho u^2)}{\partial n} = 0. \tag{19}$$

Introducing Eq.(18) and Eq.(19) into Eq.(9), the value of K is, everywhere,

$$K = \frac{\partial E / \partial n}{\partial H / \partial s} = \frac{0}{0}. \tag{20}$$

In this case, the value of K is indefinitive. We can do the following analysis. For potential flow, the total mechanical energy is uniform in the flow field everywhere, the imposed disturbance could not be amplified without an energy gradient, no matter how large the disturbance amplitude is. As the result, we conclude that potential flow (inviscid and $\nabla \times \mathrm{u} = 0$) is stable. Based on this, we obtain the following corollary:

Corollary (3): Turbulence could not be generated in potential flows.

Uniform rectilinear flow is an example of potential flow in parallel flows. For the basic cases of potential flow such as uniform flow, source/sink, free vortex, and corner flow, they are always stable.

In fact, the instability of flows is a process to make the total mechanical energy tend to becoming uniform in the flow field.

Theorem (2): Inviscid rotational ($\nabla \times \mathrm{u} \neq 0$) flow is unstable.

Proof: For inviscid flow, there is no energy loss along the streamline due to absence of viscosity. From Eqs.(15) and (16), we have

$$\frac{\partial H}{\partial s} = 0 . \tag{21}$$

The energy gradient in the transverse direction is not zero due to $\omega \neq 0$. From Eq.(14), we have

$$\frac{\partial E}{\partial n} = \frac{\partial (p + 1/2\rho u^2)}{\partial n} \neq 0 . \tag{22}$$

Introducing Eq.(21) and Eq.(22) into Eq.(9), the value of K is,

$$K = \frac{\partial E / \partial n}{\partial H / \partial s} = \infty . \tag{23}$$

It is seen that for inviscid rotational flow, the transversal energy gradient is not zero, and there is no energy loss in the streamline direction to damp the disturbance as it is an inviscid flow. Thus, any imposed finite disturbance could be amplified by the transversal energy gradient ($F = \infty$ in Eq.(8)) at sufficiently high Re. Therefore, we conclude that inviscid rotational ($\nabla \times \mathrm{u} \neq 0$) flow is unstable. This theorem has important significance for climate dynamics and meteorology, since most air flow over the atmosphere boundary layer can be treat as inviscid rotational.

For cases in which viscosity is not dominating like those not near solid walls, the flow is always unstable if it is subjected to disturbance. The non-uniform motion of air in atmosphere is an example of this kind.

Theorem (3): Velocity profile with an inflectional point is unstable when there is no work input or output to the system, for both inviscid and viscous flow, in curved streamline configurations (including parallel flow configurations).

Proof: For inviscid flow, there is no energy loss along the streamline. For viscous flow, the energy loss due to viscosity is zero at the inflection point ($(\mu\nabla^2 \mathrm{u})_s = 0$), which can be obtained from Eqs.(15) and (16), if there is no work input or output to the system (implying pressure driven flows). Thus, for both inviscid and viscous flows, we have along the streamline at the inflection point,

$$\frac{\partial H}{\partial s} = 0 . \tag{24}$$

For inviscid flow, when there is an inflection point on the velocity profile ($\partial u / \partial n \neq 0$) and if it is not at a stationary wall ($u \neq 0$), the energy gradient in the transverse direction at this point (due to rotational), from Eq.(14),

$$\frac{\partial E}{\partial n} = \frac{\partial (p + 1/2\rho u^2)}{\partial n} \neq 0 . \tag{25}$$

For viscous flow, the addition of viscosity causes diffusion by the transversal velocity (Eq.(14)). This only changes the distribution of $\partial E / \partial n$, and does not cause its value to be zero. Introducing Eq.(24) and Eq.(25) into Eq.(9), the value of K at this point is as follow,

$$K = \frac{\partial E / \partial n}{\partial H / \partial s} = \infty . \tag{26}$$

Thus, the value of the function *K* becomes infinite at the inflection point and indicates that the flow is unstable when it is subjected to a finite disturbance ($F = \infty$ in Eq.(8)). Therefore, we conclude that velocity profile with an inflectional point is unstable when there is no work input or output to the system for both viscous flow and inviscid flow. For both inviscid flow and viscous flow, we are able to prove that this is a sufficient condition for instability. If there is work input or output to the system, $\partial H / \partial s \neq 0$ at the inflection point, then this theorem is not applicable anymore. For example, the flow with an inflection point is unstable in pressure driven flows. In shear driven flows, the presence of inflection point may or may not make the flow to be unstable owing to the input of energy.

Velocity inflection could result in instability as found in experiments and simulations, e.g., the vortex instability behind a cylinder at an sufficient high Re. This phenomenon has been identified as inviscid instability [23]. According to the present theory, regardless if the flow is inviscid or viscous, inflectional velocity necessarily leads to instability. However, the fact is that viscosity does not play an important role when an inflectional instability occurs since the energy loss due to viscosity is zero at the inflection point. This theorem is also true for axisymmetrical flow in parallel flows [24]. For pressure driven flows and shear driven flows, necessary and sufficient conditions for turbulent transition have been given in [25].

4. Applications of Energy Gradient Theory

It is mentioned in previous sections that the critical value of K in Eq. (8) is decided by its maximum (K_{max}) in the field and should be a constant for parallel shear flows. In this section, we will review the comparison of the theory with the experimental data at the critical condition of turbulent transition for parallel flows and also for curved flows. The derivation of function K in Eq.(8) for pipe Poiseuille flow, plane Poiseuille flow and plane Couette flow have been given previously in [17,18, 26]. Here, we briefly give the results. The schematic diagrams of these flows are shown in Fig.1.

4.1 Pipe Poiseuille flow

For pipe Poiseuille flow, the function K has been derived in [17,18]. Here it is just introduced as,

$$K = K\left(\frac{r}{R}\right) = \frac{1}{2}\mathrm{Re}\frac{r}{R}\left(1-\frac{r^2}{R^2}\right), \tag{27}$$

where, $\mathrm{Re} \equiv \rho UD/\mu$ is the Reynolds number, ρ is the density, μ is the dynamic viscosity, U is the averaged velocity, r is in the radial direction of the cylindrical coordinate system, R is the radius of the pipe, and D the diameter of the pipe. It can be seen that K is a cubic function of radius, and the magnitude of K is proportional to Re for a fixed point in the flow field. The position of the maximum value of K occurs at $r/R=0.58$.

4.2 Plane Poiseuille flow

For plane Poiseuille flow, the function K has been derived in [17,18]. Here it is just introduced as,

$$K = K\left(\frac{y}{h}\right) = \frac{3}{4}\mathrm{Re}\frac{y}{h}\left(1-\frac{y^2}{h^2}\right). \tag{28}$$

where, $\mathrm{Re} \equiv \rho UL/\mu$ is the Reynolds number, U is the averaged velocity, y is in the transversal direction of the channel, h is the half-width of the channel, and $L=2h$ is the width of the channel. It can be seen that K is a cubic function of y which is similar to the case of pipe flow, and the magnitude of K is proportional to Re for a fixed point in the flow field. The position of the maximum value of K occurs at $y/h=0.58$. In other references, another definition of Reynolds number is also used, $\mathrm{Re} \equiv \rho u_0 h/\mu$, where u_0 the velocity at the mid-plane of the channel [2-5].

4.3 Plane Couette flow

For plane Couette flow, the function K has been derived in [26]. Here it is just introduced as,

$$K = K\left(\frac{y}{h}\right) = \mathrm{Re}\frac{y^2}{h^2}, \tag{29}$$

where $\mathrm{Re} \equiv \rho u_h h/\mu$ is the Reynolds number, u_h is the velocity of the moving plate, y is in the transversal direction of the channel, and h the half-width of the channel. It can be seen that K is a quadratic function of y/h across the channel width, and the magnitude of K is proportional to Re at any location in the flow field. The position of the maximum value of K occurs at $y/h=1.0$, and

$$K_{\max} = \frac{\rho Uh}{\mu} = \mathrm{Re}. \tag{30}$$

Table 1 Comparison of the critical Reynolds number and the energy gradient parameter K_{max} for plane Poiseuille flow and pipe Poiseuille flow as well as for plane Couette flow [17, 18].

Flow type	Re expression	Linear stability analysis, Re_c	Energy method Re_c	Experiments, Re_c	Energy gradient method, K_{max} at Re_c (from experiments), $\equiv K_c$
Pipe Poiseuille	$\mathrm{Re} = \rho UD/\mu$	Stable for all Re	81.5	2000	385 （r/R=0.58）
Plane Poiseuille	$\mathrm{Re} = \rho UL/\mu$	7696	68.7	1350	389 (y/h=0.58)
	$\mathrm{Re} = \rho u_0 h/\mu$	5772	49.6	1012	389 (y/h=0.58)
Plane Couette	$\mathrm{Re} = \rho Uh/\mu$	Stable for all Re	20.7	370	370 (y/h=1.0)

Here, U is the averaged velocity, u_0 the velocity at the mid-plane of the channel, D the diameter of the pipe, h the half-width of the channel for plane Poiseuille flow (L=2h) and plane Couette flow. The experimental data for plane Poiseuille flow and pipe Poiseuille flow are taken from Patel and Head [11]. The experimental data for plane Couette flow is taken from Tillmark and Alfredsson [27], Daviaud et al [28], and Malerud et al [29]. Here, two Reynolds numbers are used since both definitions are employed in literature. The data of critical Reynolds number from energy method are taken from [1]. For Plane Poiseuille flow and pipe Poiseuille flow, the K_{max} occurs at y/h=0.58, and r/R=0.58, respectively. For plane Couette flow, the K_{max} occurs at y/h=1.0.

The values of K_{max} at the critical condition as determined by experiments for various types of flows are shown in Table 1. We take this critical value of K_{max} for the turbulent transition as *Kc*. In Table 1, the critical Reynolds number determined from energy method is also listed in it for purpose of comparison. The critical Reynolds number determined from eigenvalue analysis of linearized Navier-Stokes equations is also listed. It is seen that the critical value of K_{max} for all the three types of flows fall within in a narrow range of 370~389. It is observed that although the critical Reynolds number is different for these flows, the critical value of K_{max} is the same for these flows. This demonstrates that K_{max} as a dominating parameter provides certain degree of consistency for the transition to turbulence. These data strongly support the proposed method in the present study and the claim that the critical value of K_{max} is constant for all parallel flows, as discussed before. In comparison, the critical Reynolds number predicted by the energy method based on Reynolds-Orr equation is much lover than the experimental data for all the three cases. While the linear stability analysis lacks the physical mechanism behind turbulent transition and therefore it is unable to predict the critical condition of turbulent transition.

The location of K_{max} represents the position where the flow instability is first initiated if the disturbance is uniformly distributed as shown in Eq.(8). For pipe flow, the experiments by Hof et al. [30] showed that the streamwise vortices at Re=2000 (the base flow is still laminar) occur at about *r/R*=0.5-0.6 (see their Fig.2(A) in [30]), which accords with the present study where we have found the maximum of *K* occurring at the ring of *r/R*=0.58 [17,18]. Nishi et al [20] did experiment on turbulent transition for pipe flow through puffs and slugs generation and the disturbance was introduced at the pipe inlet by a short duration of inserted "wall fences". Figures 6 and 7 show an example of the experimental results chosen from a large number of time records for the instantaneous velocities of the puffs at different radial locations r/R. These pictures indicate that the flow becomes most unstable in the range of r/R=0.47-0.73 under the disturbance influence, which is in agreement with the prediction in this study that the r/R=0.58 is the most unstable position for initiation of transition.

For plane Poiseuille flow, the position of the maximum of *K* occurs at *y/h=0.58* so that this position is the most dangerous position for instability. Nishioka et al's experimental data has shown that the flow oscillation first appears at the location of about *y/h=0.6* [19]; see Fig.5.

For plane Couette flow, the position of the maximum of *K* occurs at *y/h=1.0.* Owing to the fact of no-slip at the wall, the disturbance at the wall is zero. The most dangerous position should be off a short distance from the wall such that the magnitude of the disturbance is apparently playing a role and the value of *K* is still large. Thus, the value of *F* could get large value and, therefore, the Eq.(8) is violated. Some nonlinear analysis showed that the development of disturbance and the distortion of base flow first start at the layer near one of the walls [31]. However, from Eq.(8), this most dangerous location also depends on the distribution of disturbance, especially the wave number.

4.4 Taylor-Couette flow

The energy gradient theory has been applied to Taylor-Couette flow between concentric rotating cylinder and it is confirmed that this method is also applicable to rotating curved flows if the kinetic energy in parallel flows is replaced by the total mechanical energy (Eq.(9), kinetic energy plus pressure energy while gravitational energy is neglected) [32]. The mechanism of energy loss enhancing flow stability has been studied for both plane Couette flow and Taylor-Couette flow in [22].

The results from energy gradient theory have been compared with the available experimental data for Taylor-Couette flow between concentric rotating cylinders, and excellent agreement has been obtained [32]. Here, some examples are given in Fig.8 and Fig.9. In the figure, for the occurrence of primary instability (uniform laminar flow becomes cell pattern of rolls), the critical value of K_{max} is a constant for a given geometry independent of the rotating speeds of the two cylinders as observed from experiments. The critical value of K_{max} is observed from the experiments at the condition of occurrence of primary instability for the case of the inner cylinder rotating and the outer cylinder set to rest. These results confirm that the proposed theory is also applicable to rotating flows.

It should be pointed out that the primary instability in Taylor-Couette flow between concentric rotating cylinders is a case of transition of laminar flow to laminar flow. This flow can be exactly predicted by the linear stability theory with infinite small disturbance [3-5].

4.5 Annulus flow

The critical condition for turbulent transition in annulus flow has been calculated with the energy gradient method for various radius ratios. The critical flow rate and critical Reynolds number are given for various radius ratios. Then, the analytical results are compared with the experiments in the literature [33]. Finally, the implication of the result is discussed in terms of the drag reduction and mixing as well as heat transfer in practical industrial applications of various fluid delivery devices.

The critical Reynolds number for the flow in an annulus is obtained as,

$$\mathrm{Re}_c = \frac{U\rho 2(R-R_1)}{\mu} = \frac{2K_c}{f^*_{\max}}\left(1-\frac{R_1}{R_2}\right)\left[\left(1+k^2\right)-\frac{\left(1-k^2\right)}{\ln(1/k)}\right], \tag{31}$$

where $f^*_{\max}$ is the maximum of the following function f in the flow field,

$$f\left(\frac{r}{R},k\right)=\left[1-\left(\frac{r}{R}\right)^2+b\ln\frac{r}{R}\right]\left[\frac{r}{R}-\frac{b}{2(r/R)}\right]. \tag{32}$$

It is found that the magnitude of f is large on the side of inner cylinder than that of the outer cylinder. Thus, the flow state on the inner cylinder side determines the critical condition of turbulent transition. The critical condition of the theoretical result is compared with experiments in Fig.10 for the turbulent transition at the side of the inner cylinder. It is found that there is very good agreement. In the reference, turbulent transition is marked by a sudden increase of the drag coefficient.

It is shown that the critical Reynolds number for onset of turbulent transition increases with the radius ratio of the annulus (k). It reaches to the critical Re of circular pipe flow at the radius ratio of about k<0.12~0.18, where the radius of the pipe is same as the outer radius of the annulus. It is clear from Fig.10 that the inner cylinder creates instability for k<0.12~0.18; and enhance stability for k>0.12~0.18. Following this principle, the flow transition can be controlled by changing the radius ratio for a given outer radius. The idea can be employed in the design of fluid flow devices to control the flow status like drag reduction (by keeping to laminar flow) or increase the mixing of the fluid media and the heat transfer (by changing to turbulent flow).

The critical value of Re in plane Poiseuille flow obtained by extrapolating the data of annulus flow to k=1, is perfectly consistent with the experimental data. This result confirms that the energy gradient method is applicable for pipe Poiseuille flow, plane Poiseuille flow as well as annulus flow for turbulent transition.

4.6 Boundary Layer flow

The energy gradient method is successfully employed to analyze the flow instability and turbulent transition in boundary layer flows [34]. It is found that the maximum of the energy gradient function occurs at the wall for the Blasius boundary layer flow (Fig.11). At this location under a sufficiently high Reynolds number, Re_x, the stability criterion is first violated very near the wall at even very small perturbation level. This event serves as the origin of self-sustenance of wall turbulence. In comparison, in Poiseuille flows, a much larger disturbance is always needed to sustain the transition since the value of K is finite. The mechanism of receptivity to free-stream turbulence can be understood from the energy gradient criterion. That is, the free-stream disturbance can propagate towards the wall by the "energy gradient" process to cause turbulent transition, and the transition point in the boundary layer can be moved forward towards the leading edge when the level of external disturbance increases.

5. Prediction of Turbulent Transition

There is no fundamental prediction method available for turbulent transition. In engineering, people use correlations based on experiments to predict the onset of turbulent transition. Currently, there are four approaches to predict turbulent transition which are only for boundary layer flows. For internal flows, there is no any consistent correlation [35].

5.1 Empirical method

(a) Michel's Method (1952): This method is based on local values of momentum thickness and position [36]. The momentum thickness of boundary layer can be calculated by Thwaies' method or other similar methods. That is

$$\mathrm{Re}_{\theta,tr}=\frac{U(x)\theta(x)}{\nu}\approx 2.9\,\mathrm{Re}_{x,tr}^{\ 0.4}. \tag{33}$$

(b) Cebeci and Smith Method (1974):

$$\mathrm{Re}_{\theta,tr}\approx 1.174\left[1+\left(\frac{22{,}400}{\mathrm{Re}_{\theta,tr}}\right)\right]\mathrm{Re}_{x,tr}^{\ 0.46}. \tag{34}$$

This equation is for $0.1\times10^6\le \mathrm{Re}_x\le 40\times10^6$ [37]. This equation is correlated with the e^n method for n=9.

(c) Mayle's formulation [38]:

$$\mathrm{Re}_{\theta,tr}=400Tu^{-5/8}. \tag{35}$$

Here, $Tu=\frac{1}{U_0}\left[\frac{1}{3}\left(\overline{u'^2}+\overline{v'^2}+\overline{w'^2}\right)\right]^{1/2}$ is the disturbance of free-stream.

(d) Abu-Ghannam and Shaw formulation[39]:

$$\mathrm{Re}_{\theta,tr} = 163 + \exp\left[F(A) - \frac{F(A)}{6.91} Tu \right], \tag{36}$$

$$F(A) = 6.91 + 12.75H + 63.64H^2 \quad for \quad H < 0$$
$$F(A) = 6.91 + 2.48H - 12.27H^2 \quad for \quad H > 0.$$

Here, H is the shape parameter of the boundary layer.

(e) Proposed semi-empirical formula for pipe flow: These empirical formulas mentioned above are only for boundary layer flow. For pipe flow, a new equation is proposed in this study based on the energy gradient theory, i.e., using Eq.(12) and Fig.4. That is

$$\mathrm{Re}_c = 12.8\,(v'_m / U)^{-1}, \text{ for } \mathrm{Re} \geq 2000. \tag{37}$$

This equation is only suitable for transverse injection disturbance for pipe flow. If the disturbance is not along the transverse direction, it is not valid.

(f) Prediction of the minimum critical Re for parallel flows: According to the present theory (Energy gradient theory), the critical value of $K_{\max}$ for turbulent transition is about 380 in parallel flows. Thus, for a parallel flow, if we set the critical value $K_c = 380$, the minimum critical value of Re for turbulent transition can be predicted, as in [33]. In this process, the value of K in the flow field can be calculated by analytical solution or numerical solution. For non-parallel flows, the critical value of $K_{\max}$ depends on the geometry and the curvature of streamlines. For obtaining a correlation of K_c with the curvature of streamlines, much experimental data are needed. For primary instability of the base laminar flow occurring in Taylor-Couette flow, this correlation has been available [32].

5.2 The e^n Method

Smith and Gamberoni [40] and van Ingen [41] independently developed the so-called e^n method which is widely used in aircraft design and other applications. This method is based on linear stability theory from Orr-Sommerfeld equation. For two-dimensional flow, the disturbances are amplified or damped according to the sign of the spatial growth rate of $-\alpha_i$. For a given mean flow, the stability diagram can be calculated by the solution of Orr-Sommerfeld equation [42,35]. Let us consider a disturbance wave which propagates downstream with a fixed frequency f_1, see Fig.12. This wave will be amplified when it passes through the instability zone from x_0 to x_1. At a given position x, the total amplification rate can be calculated as

$$\frac{A}{A_0} = \exp\left[\int_{x_0}^{x} -\alpha_i dx\right]. \tag{38}$$

The envelope of the total amplification curves is

$$n = \max\left[\ln(A / A_0\right], \text{ for } f_1, f_2, f_3, \ldots. f_m. \tag{39}$$

Generally, it is assumed that transition will occur if the n factor reaches a critical value of 7~10. However, it should be pointed out that this method is only suitable for the cases of low disturbances since it is based on linear stability analysis.

5.3 RANS-γ method

This method relies on the solution of an equation for the intermittent factor in the transition zone [43-47]. This equation can be an intermittency transport equation or an algebraic equation of intermittency. This equation is coupled with the Reynolds averaged Navier-Stokes (RANS) equations, while appropriate turbulent model is needed. In the transition region, the effective viscosity μ_{eff} is composed of the turbulent eddy viscosity μ_t and the non-turbulent viscosity μ_{nt} such that

$$\mu_{eff} = (1-\gamma)\mu_{nt} + \gamma\mu_t. \tag{40}$$

For boundary layer flow on a flat plate, it has obtained very good agreement with experiment (see Fig.13). In a recent study, this method has been successfully used in transition prediction on rotors. More recently, Minkowycz et al [48] simulated the turbulent transition in a channel flow using the intermittency transport equation method. The effect of inlet conditions on the downstream flow is the main focus.

5.4 Direct numerical simulation (DNS) method

Direct numerical simulation using Navier-Stokes equations for turbulent transition is the most reliable method for capturing the transition process [49-55]. However, this method is only available for some simple configurations, and it has not been yet extended to engineering applications due to its requirement of huge CPU resources. For boundary layer flow, plane Poiseuillel flow and plane Couette flow, several DNS works have been done. For plane Couette flow, the process of amplification of turbulent spot has been observed [54, 55]. The critical Re obtained by DNS accords well with the experiments.

Figures 14 and 15 show the results of DNS for plane Couette flow with two walls moving in opposite directions [54]. For Re=320, a wave packet stimulated by an imposed disturbance decays. For Re=375, the wave packet amplifies with time evolution and it transits to turbulent spot in downstream. Thus, it can be commented that turbulent transition occurs at about Re=320~375. This is in agreement with the experimental results which showed Rec=370 [27-29], and previous result of direct numerical simulation with Rec=375 [55]. These results demonstrated that DNS is a powerful tool for simulating the turbulent transition.

6. Conclusions

The energy gradient method for curved flows is proposed in this study for flow instability and turbulent transition. Criterion of stability is derived in detail which shows that the stability of a flow depends on the Re and the disturbance amplitude. Excellent agreement has been obtained between the theory and the experimental data for various flows, including the turbulent transition in parallel flows and the primary instability in the Taylor-Couette flows. Based on the proposed theory, several basic theorems for flow instability in general cases are provided for the first time. The flowing conclusions can be drawn:

(1) The energy gradient theory is valid for both parallel flows and curved flows.

(2) There may be a universal mechanism for various turbulent transitions occurring in nature and engineering, i.e., the energy gradient mechanism.

(3) The basic theorems for flow instability proofed are in consistent with the observations. It is believed that these theorems have significant importance to the study of flow stability and turbulent transition.

The energy gradient theory is also demonstrated to be suitable for non-Newtonian flows where instability occurs at zero Re, but elastic effect dominates the stability of the flow [56, 57].

Nomenclature

A	amplitude of disturbance in transverse direction m
b	$b=(1-k^2)/\ln(1/k)$ in annulus flow
D	diameter of the pipe for pipe flow m
E	total mechanical energy of unit volume of fluid J m^{-3}
h	half-channel width in plane Couette flow and plane Poiseuille flow m
H	total mechanical energy loss of unit volume of fluid due to viscosity in streamwise direction J m^{-3}
k	radius ratio in annulus flow
K	function of coordinates (dimensionless).
K_c	critical value of K_{max} for instability (dimensionless).
K_{max}	maximum of K in the domain (dimensionless).
l	streamwise length of a half-period m
m	mass of fluid kg
n	coordinate in transverse direction m
P	static pressure N m^{-2}
Q	volume of fluid m^3
r	radius in annulus flow m
R	radius of outer cylinder in pipe flow and annulus flow m
R_1	radius of inner cylinder in annulus flow m
Re	Reynolds number (dimensionless).
s	coordinate in streamwise direction m
t	time s
T	period of wave s
u	velocity component in the main flow direction m s^{-1}
u_0	velocity at the mid-plane for plane Poiseuille flow (channel flow) m s^{-1}
U	average velocity in the flow passage m s^{-1}
v	velocity component in the transverse direction m s^{-1}
v'_m	$=A\omega$, amplitude of the disturbance of velocity in transverse direction m s^{-1}
W	work done to the unit volumetric fluid by external J m^{-3}
x	coordinate in the streamwise direction m
y	coordinate in the transverse direction m
μ	dynamic viscosity Nm^{-2} s
ν	kinematic viscosity m^{2}s^{-1}
ρ	density of fluid kg m^{-3}
ω	frequency of disturbance rad s^{-1}
θ	momentum thickness of boundary layer m

References

[1] P.J.Schmid, and D.S. Henningson, “Stability and transition in shear flows,” New York, Springer-Verlag, 2000.

[2] C.C.Lin, “The theory of hydrodynamic stability,” Cambridge, Cambridge Press, 1955.

[3] R. Betchov, W.O.J. Criminale, “Stability of parallel flows,” New York, Academic Press, 1967.
[4] P.G. Drazin, W.H. Reid, “Hydrodynamic stability,” Cambridge University Press, Cambridge, England, 1981.
[5] D.D. Joseph, “Stability of fluid motions,” Vol. 1 and 2, Berlin, Springer-Verlag, 1976.
[6] L. Rayleigh, “On the stability or instability of certain fluid motions,” Proc. Lond. Maths. Soc., 11, 1880, pp. 57-70.
[7] W.M. Orr, “The stability or instability of the steady motions of a perfect liquid and of a viscous liquid,” Proc. Royal Irish Academy, A27, 1907, pp. 9-138.
[8] J.T. Stuart, “Nonlinear Stability Theory,” Annu. Rev. of Fluid Mech., 3, 1971, pp. 347-370.
[9] B.J. Bayly, S.A. Orszag, T. Herbert, “Instability mechanism in shear-flow transition,” Annu. Rev. Fluid Mech., 20, 1988, pp. 359-391.
[10] O. Reynolds, “An experimental investigation of the circumstances which determine whether the motion of water shall be direct or sinuous, and of the law of resistance in parallel channels,” Phil. Trans. Roy. Soc. London A, 174, 1883, 935-982.
[11] V.C. Patel, M.R. Head, “Some observations on skin friction and velocity profiles in full developed pipe and channel flows,” J. Fluid Mech, 38, 1969, pp. 181-201.
[12] L.N. Trefethen, A.E. Trefethen, S.C. Reddy, T.A. Driscoll, “Hydrodynamic stability without eigenvalues,” Science, 261, 1993, pp. 578-584.
[13] A.G. Darbyshire, T. Mullin, “Transition to turbulence in constant-mass-flux pipe flow,” J. Fluid Mech, 289, 1995, pp. 83-114.
[14] S.J. Chapman, “Subcritical transition in channel flows,” J. Fluid Mech., 451, 2002, pp. 35-97.
[15] B. Hof, A. Juel, T. Mullin, “Scaling of the turbulence transition threshold in a pipe,” Phys. Rev. lett., 91, 2003, 244502.
[16] J. Peixinho and T. Mullin, “Finite-amplitude thresholds for transition in pipe flow,” J. Fluid Mech., 582(2007), pp. 169-178.
[17] H.-S. Dou, “Mechanism of flow instability and transition to turbulence,” International Journal of Non-Linear Mechanics, 41(2006), 512-517. http://arxiv.org/abs/nlin.CD/0501049.
[18] H.-S. Dou, “Physics of flow instability and turbulent transition in shear flows,” Technical Report of National University of Singapore, 2006; http://arxiv.org/abs/physics/0607004. Also as part of the invited lecture: H.-S. Dou, “Secret of Tornado,” International Workshop on Geophysical Fluid Dynamics and Scalar Transport in the Tropics, NUS, Singapore, 13 Nov. - 8 Dec., 2006.
[19] M. Nishioka, S. IIda, Y. Ichikawa, “An experimental investigation of the stability of plane Poiseuille flow,” J. Fluid Mech., 72, 1975, pp. 731-751.
[20] M. Nishi, B. Unsal, F. Durst, G. Biswas, “Laminar-to-turbulent transition of pipe flows through puffs and slugs,” J. Fluid Mech., 614, 2008, pp. 425-446.
[21] H-S. Dou, “Three important theorems for flow stability,” Proceedings of the Fifth International Conference on Fluid Mechanics, Ed. by F. Zhuang and J. Li, Tsinghua University Press & Springer, 2007, pp. 57-60.
[22] H.-S. Dou, B.C. Khoo, K.S.Yeo, “Energy loss distribution in the plane Couette flow and the Taylor-Couette flow between concentric rotating cylinders,” Inter. J. of Thermal Science, Vol.46, 2007, pp. 262-275.
[23] C H K Williamson, “Vortex dynamics in the cylinder wake,” Annu. Rev. Fluid Mech., 28, 1996, pp. 477-539.
[24] H.-S. Dou, “Viscous instability of inflectional velocity profile,” Proceedings of the Forth International Conference on Fluid Mechanics, Ed. by F. Zhuang and J. Li, Tsinghua University Press & Springer-Verlag, July 20-23, 2004, Dalian, China, pp. 76-79.
[25] H.-S. Dou, B.C. Khoo, “Criteria of turbulent transition in parallel flows,” Modern Physics Letters B, Vol. 24, No.13, May 2010, pp. 1437-1440.
[26] H.-S. Dou, B.C. Khoo, “Investigation of Turbulent transition in plane Couette flows Using Energy Gradient Method,” Advances in Appl. Math. and Mech., 3(2), 2011, pp.165-180.
[27] N. Tillmark, P.H. Alfredsson, “Experiments on transition in plane Couette flow,” J. Fluid Mech., 235, 1992, 89 –102.
[28] F. Daviaud, J. Hegseth, P. Bergé, “Subcritical transition to turbulence in plane Couette flow,” Phys. Rev. Lett., 69, 1992, pp. 2511-2514.
[29] S. Malerud, K.J. Mölfy, W.I. Goldburg, “Measurements of turbulent velocity fluctuations in a planar Couette cell,” Phys. Fluids, 7, 1995, pp. 1949-1955.
[30] B. Hof, C.W. H. van Doorne, J. Westerweel, F.T. M. Nieuwstadt, H.Faisst, B.Eckhardt, H.Wedin, R.R. Kerswell, F.Waleffe, “Experimental observation of nonlinear traveling waves in turbulent pipe flow,” Science, 305 (2004), No.5690, pp. 1594-1598.
[31] M. Lessen, M.G. Cheifetz, “Stability of plane Coutte flow with respect to finite two-dimensional disturbances,” Phys. Fluids, 18, 1975, pp. 939-944.
[32] H.-S. Dou, B.C. Khoo, K.S. Yeo, “Instability of Taylor-Couette Flow between Concentric Rotating Cylinders,” Inter. J. of Therm. Sci., 47, 2008, 1422-1435.
[33] H.-S. Dou, B.C. Khoo, H.M. Tsai, “Determining the critical condition for turbulent transition in a full-developed annulus flow,” Journal of Petroleum Science and Engineering, 73 (1-2), 2010, pp. 41-47.
[34] H.-S. Dou, B.C. Khoo, “Mechanism of wall turbulence in boundary layer flows,” Modern Physics Letters B, 23 (3), 2009, 457-460. http://arxiv.org/abs/0811.1407.
[35] F. M. White, “Viscous Fluid Flow,” 2nd Edition, 1991, MacGraw, New York, pp. 335-393.
[36] R. Michel, “Study of transition on wing sections; establishment of a criterion for the determination of point of transition and calculation of the wake of an incompressible profile,” 1952, ONERA Report 1/1578A (in French).
[37] T. Cebeci, A. M. O. Smith, “Analysis of Turbulent Boundary Layers,” 1974, Academic Press, New York.
[38] R. E. Mayle, “The 1991 GTI Scholar Lecture: The Role of Laminar–Turbulent Transition in Gas Turbine Engines,” ASME J. Turbomachery, 113, 1991, pp. 509-537.
[39] B.J. Abu-Ghannam, and R. Shaw, “Natural Transition of Boundary Layers-The Effect of Turbulence,” Pressure Gradient and Flow History, J. Mech. Eng. Sci., 22, No. 5, 1980, pp. 213-228.
[40] A.M.O. Smith and N. Gamberoni, “Transition, pressure gradient and stability theory,” Pept.ES 26388, Douglas Aircraft Co., El Segundo, California, 1956.
[41] J. L. van Ingen, “A suggested semi-empirical method for the calculation of boundary layer transition region,” Rept. UTH-74,

Univ. of Techn., Dept. of Aero. Eng., Deft, 1956.
[42] D. Arnal, “Control of laminar-turbulent transition for skin friction drag reduction,” In: Control of Flow Instabilities and Unsteady Flows,”\ Eds. G.E.A.Meier and G.H.Schnerr, Springer, 1996, New York, 118-153.
[43] F.R.Menter, R.B.Langtry, S.Volker, “Transition modelling for general purpose CFD codes,” Flow Turbulence Combust, 2006, 77: 277-303.
[44] Y. B. Suzen, and P.G.Huang, “Modeling of flow transition using an intermittency transport equation,” J. Fluids Engineering, 122,2000, pp. 273-284.
[45] Y. Lian, and W. Shyy, “Laminar-Turbulent Transition of a Low Reynolds Number Rigid or Flexible Airfoil,” AIAA J., 45(7), 2007, pp. 1501-1513.
[46] N.N. Sorensen, “CFD modeling of laminar-turbulent transition for airfoils and rotors using the $\gamma - \mathrm{Re}_\theta$ model,” Wind Energy, 12,2009, pp. 715-733.
[47] L. Wang and S. Fu, “Modelling flow transition in a hypersonic boundary layer with Reynolds-averaged Navier-Stokes approach,” Science in China Series G: Physics, Mechanics & Astronomy, 52, 2009, pp. 768-774.
[48] W.J. Minkowycz, J. P. Abraham, E. M. Sparrow, “Numerical simulation of laminar breakdown and subsequent intermittent and turbulent flow in parallel-plate channels: Effects of inlet velocity profile and turbulence intensity,” Inter. J. Heat and Mass Transfer, 52(2009), pp. 4040-4046.
[49] P. Moin, and K. Mahesh, “Direct numerical simulation: A tool in turbulent research,” Annu. Rev. Fluid Mech., 30, 1998, pp. 539-578.
[50] L. Kleiser, and T. A. Zang, “Numerical simulation of transition in wall-bpounded shear flows,” Annu. Rev. Fluid Mech., 23, 1991, pp. 495-537.
[51] H. Shan, Z. Zhang, F.T.M. Nieuwstadt, “Direct numerical simulation of transition in pipe flow under the influence of wall disturbances,” Inter. J. of Heat and Fluid Flow, 19, 1998, pp. 320-325.
[52] X. J. Wang, J.S. Luo, H. Zhou, “Inherent mechanism of “breakdown” process during laminar flow-turbulence transition in channel flows,” Science in China Ser. G, 35(1), 2005, pp. 71-78 (In Chinese).
[53] K. S. Yeo, X. Zhao, Z. Y. Wang and K. C. Ng , “DNS of wavepacket evolution in a Blasius boundary layer,” Journal of Fluid Mechanics, 652, 2010, pp. 333-372.
[54] H.-S. Dou and B. C. Khoo, “Parallel direct numerical simulation of turbulent transition using full Navier-Stokes Equations,” Technical Report, National University of Singapore, Nov. 2009.
[55] A. Lundbladh, A. Johansson, “Direct simulation of turbulent spots in plane Couette flow,” J. Fluid Mech., 229, 1991, 499-516.
[56] H.-S. Dou, and N. Phan-Thien, “An Instability Criterion for Viscoelastic Flow Past A Confined Cylinder,” Korea and Australia Rheology, 20, 2008, pp. 15-26.
[57] H.-S. Dou, and N. Phan-Thien, “Viscoelastic flows around a confined cylinder, Part one: Instability and velocity inflection,” Chemical Engineering Science, 62 (15), 2007, pp. 3909-3929.

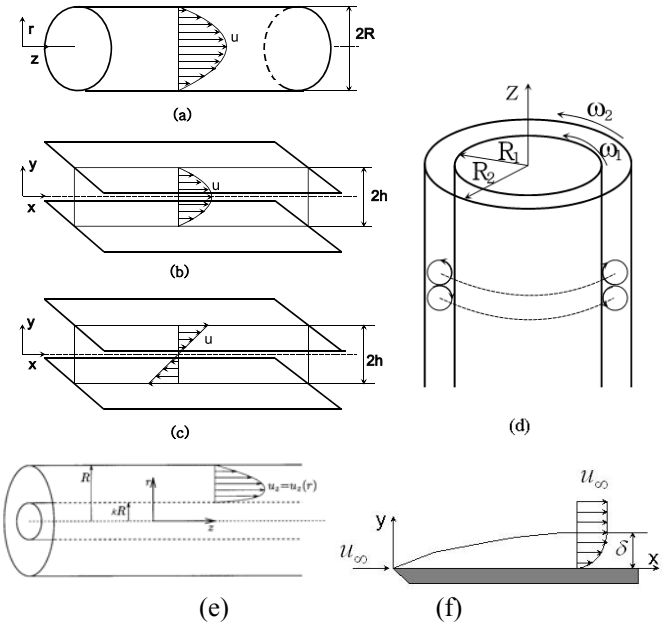

Fig. 1 Schematic of wall bounded parallel flows. (a) Pipe Poiseuille flow; (b) Plane Poiseuille flow; (c) Plane Couette flow; (d) Taylor-Couette Flow; (e) Annulus Flow; R_2=R; R_1=kR. (f) Boundary layer flow.

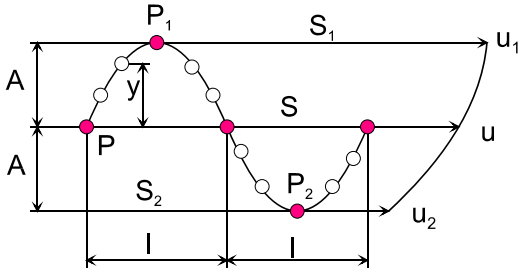

Fig. 2 Movement of a particle around its original equilibrium position in a cycle of disturbance for parallel flows.

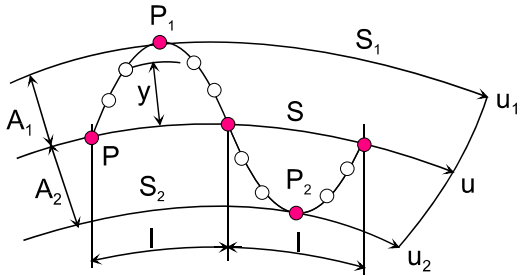

Fig. 3 Movement of a particle around its original equilibrium position in a cycle of disturbance for curved flows.

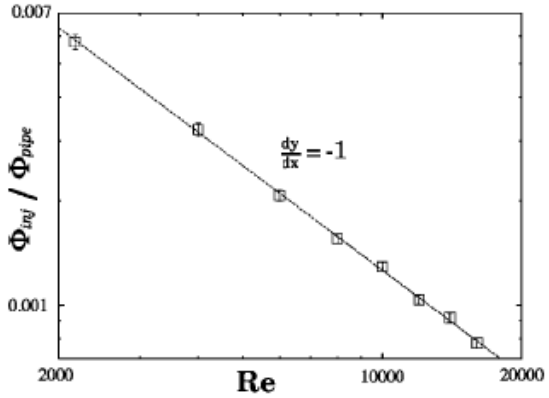

Fig. 4 Experimental results for pipe flow: the normalized flow rate of disturbance versus the Reynolds number (Hof, Juel, and Mullin, 2003). The range of Re is from 2000 to 18,000. The normalized flow rate of disturbance is equivalent to the normalized amplitude of disturbance for the scaling of Reynolds number, $\Phi_{inj} / \Phi_{pipe} \sim (v'_m / U)_c$.

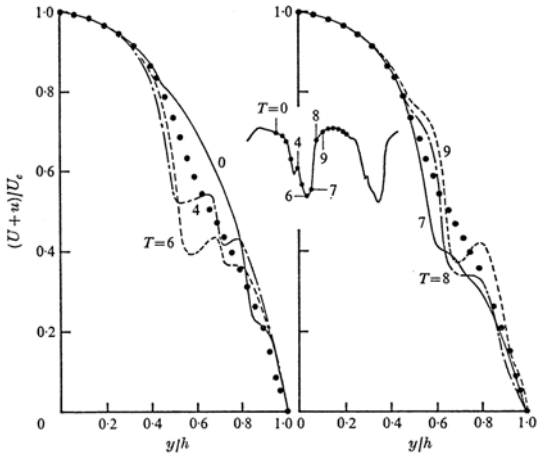

Fig. 5 Experimental data for channel flow indicate that instability first occurs at y/h=0.5-0.62, Nishioka et al (1975).

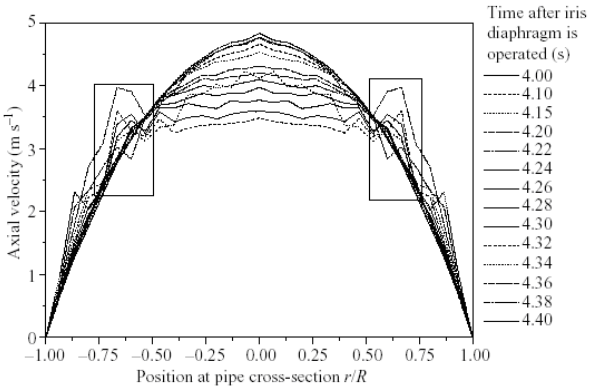

Fig. 6 Axial velocity as a function of different radial position r/R at different time after the iris diaphragm is operated at Re=2450, reproduced from Nishi et al (2008) (Courtesy of F. Durst;). The oscillation first started in r/R=0.53~0.73.

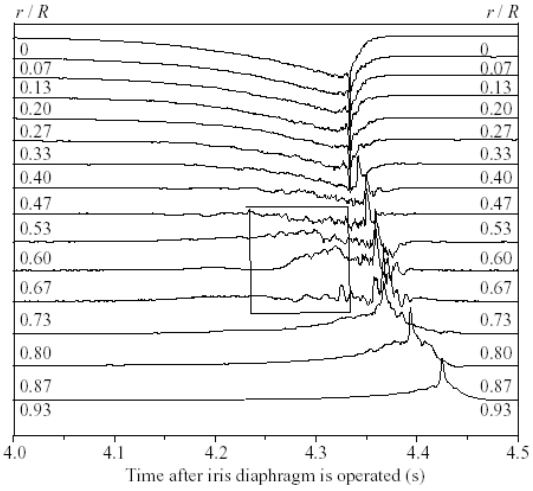

Fig. 7 Axial velocity at different radial position r/R vs. time which is shown from the time when the iris diaphragm is operated at Re=2450, reproduced from Nishi et al (2008) (Courtesy of F. Durst; Use permission by Cambridge University Press). The oscillation first started in r/R=0.53~0.73.

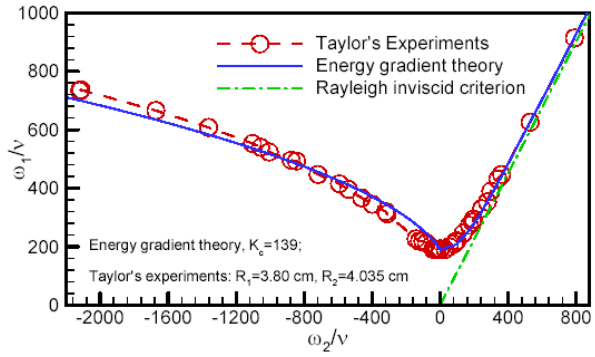

Fig. 8 Comparison of the theory with the experimental data for the instability condition of Taylor-Couette flow (Taylor (1923)'s experiments, R1=3.80 cm, R2=4.035 cm). The relative gap width is h/R_i=0.06184.

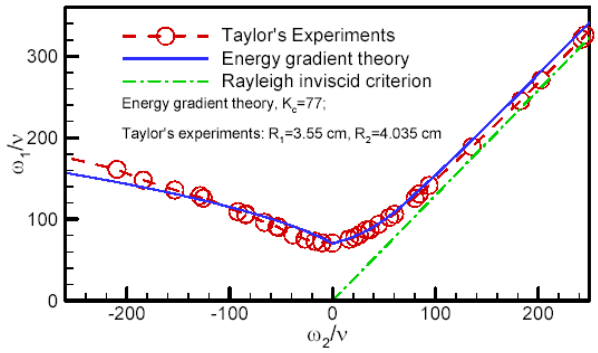

Fig. 9 Comparison of the theory with the experimental data for the instability condition of Taylor-Couette flow (Taylor (1923)'s experiments, R1=3.55cm, R2=4.035 cm). The relative gap width is h/R_i=0.1366.

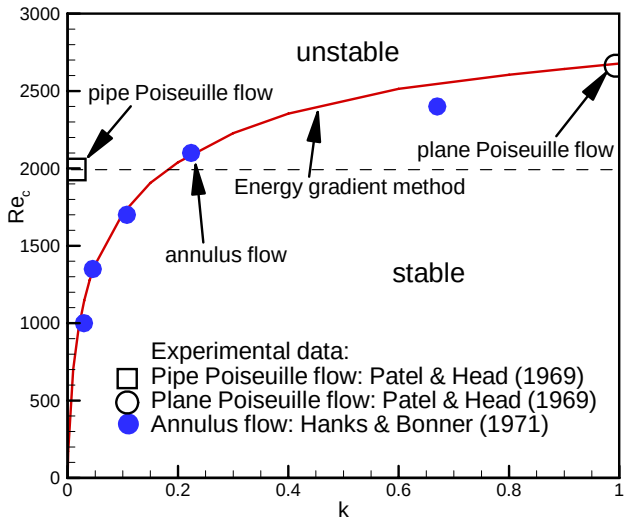

Fig. 10 Comparison of prediction with experimental data for turbulent transition at the inner cylinder: Reynolds number at critical condition of inner cylinder for annulus flow versus the radius ratio k [33]. The out radius is kept constant. The data at k=0 means the case for circle pipe flow. The data at k=1 corresponds to the case for plane Poiseuille flow.

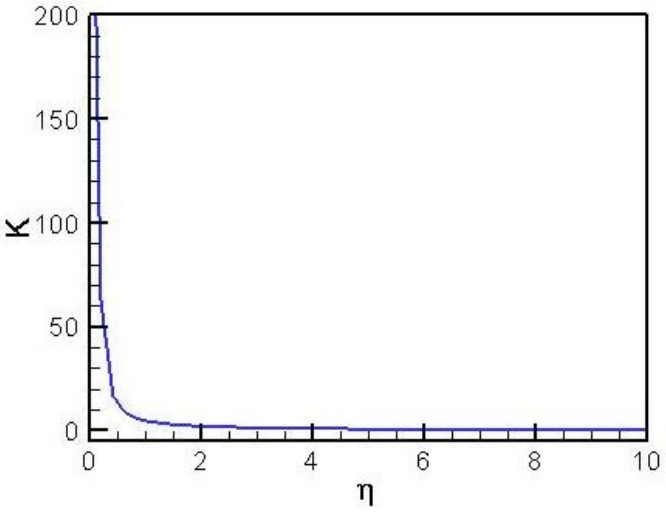

Fig. 11 Distribution of *K* versus the transverse direction for boundary layer flow [34]. The value of K approaches infinite approaching the wall. Thus, even a very small disturbance can trigger the flow to transit to turbulence near the wall, according to Eq.(8). In experiments, it looks like that turbulence is originated from the wall region.

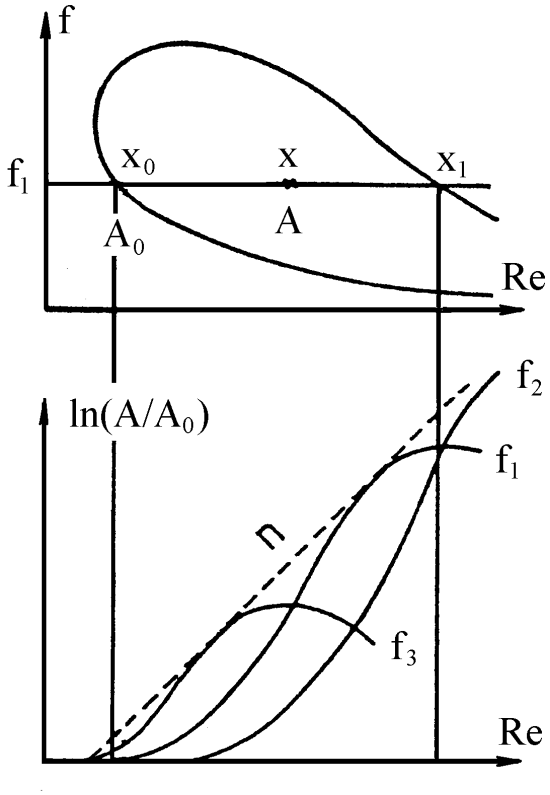

Fig. 12 Prediction of the e^n method. Stability diagram of linear stability (top) and amplification factor n envelope (bottom), adapted from Arnal (1996).

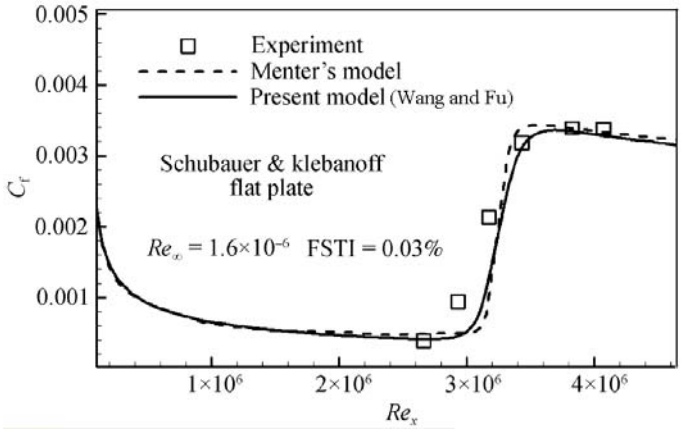

Fig. 13 Comparison of the skin friction predicted with experiment (adapted from Wang and Fu, 2009).

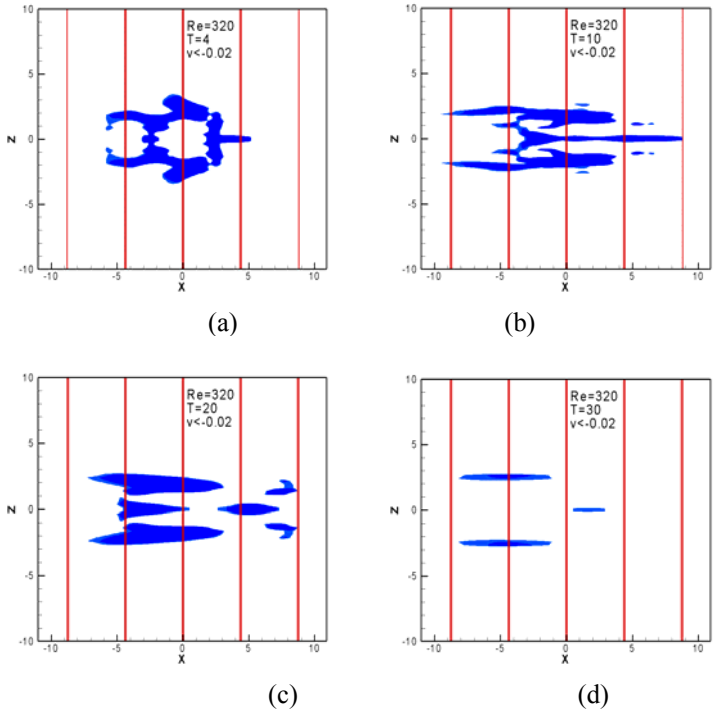

Fig. 14 Simulation of turbulent transition for plane Couette flow at Re=320 [54]. Turbulent spot decays with time development. The time is non- dimensionalized.

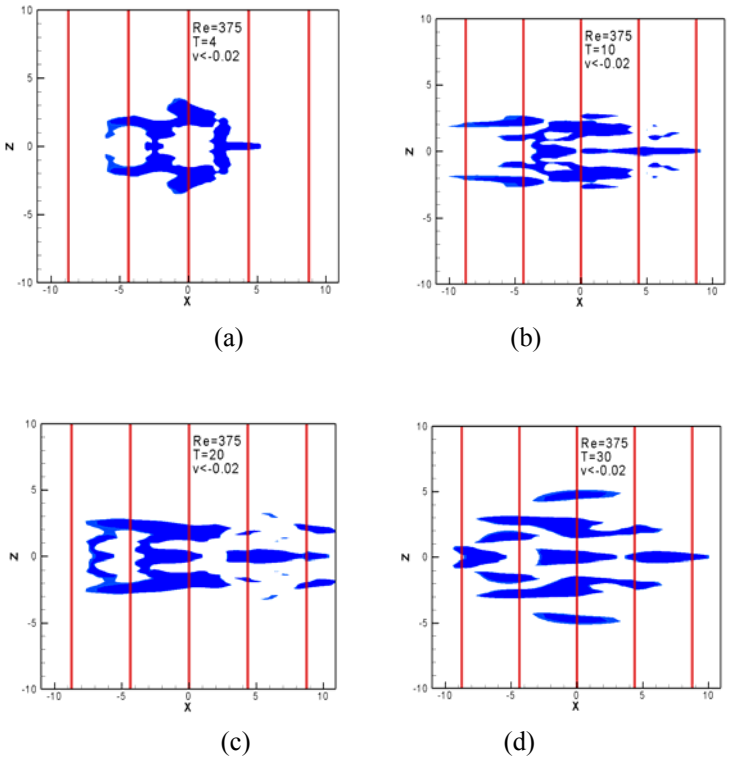

Fig. 15 Simulation of turbulent transition for plane Couette flow at Re=375 [54]. Turbulent spot enlarges with time development. The time is non- dimensionalized.